Application of Coupled Map Lattice as an Alternative to Classical Finite Difference Method for Solving the Convection-Diffusion Boundary Value Problem

Lukasz Korus
Department of Control Systems and Mechatronics
Wroclaw University of Science and Technology
Janiszewskiego 11/17
Wroclaw, 50-370, Poland

This paper presents a mathematical model for a piston flow reactor based on the material balance law using partial differential equations. A more general, nondimensional variant of the model is also derived. The finite difference method and coupled map lattice are used to create numerical algorithms to simulate spatio-temporal behavior in the studied system. The paper also includes a stability analysis of the proposed algorithms and results of numerous numerical simulations, done in order to compare both methods and to visualize the spatio-temporal behavior of the reactor and the effects of different model parameters. Discussion of the obtained results and comparison of both algorithms is also provided.

Keywords: piston flow reactor; plug flow reactor; distributed parameter systems; coupled map lattice

1. Introduction

This paper tackles the issue of numerical solution of the convection-diffusion boundary value problem using the finite difference method (FDM) as well as the heuristic coupled map lattice (CML) method. The boundary value problem describes the dynamics of the tubular chemical reactor, where one kind of mass is transformed into another during a chemical reaction. The main goal of the paper is a qualitative, simulation-based comparison of these two different numerical discretization schemes for the evaluation of the given partial differential equation (PDE). Moreover, a stability analysis of both methods is also conducted in order to prove their capabilities for practical implementation. While application of partial differential equations (PDEs) to build mathematical models of complex distributed parameter systems (DPSs) is well known and widely described in literature (e.g., [1–3]), using CML to simulate complex behavior of the piston flow

https://doi.org/10.25088/ComplexSystems.30.1.47

reactor (PFR) seems to be a rather new direction. The original contribution of this paper is an application of the heuristic CML method to numerically solve the complex PDE.

The issue of distributed parameter system (DPS) modeling is crucial, because by conducting different numerical simulations, a better understanding of their spatio-temporal behaviors can be achieved [4–6]. A number of physical objects can be described as distributed systems. In practice, this means some of their parameters and signals should be considered functions of both temporal and spatial independent variables [7]. Different examples of such systems can be found in the field of electrics [8, 9], mechanics [5], fluid dynamics [10, 11], biology [12–14] and chemistry [2, 15–19].

Obviously, modeling is only one of the aspects addressed in the literature for such systems. Additional, optimal types of experimental design, including the identification of distributed systems, are widely discussed as well [20–25]. Moreover, since many DPSs demonstrate chaotic spatio-temporal behavior, issues of describing such behaviors quantitatively and qualitatively are also dealt with [26–28]. Furthermore, a great deal of effort and attention is put into control algorithms, which optimize defined quality factors [29] or stabilize chaotic behavior [30–33].

Mathematical models of DPSs are typically formulated as PDEs [3, 34], but for some applications, cellular automata (CAs) [35–37] or CML [38–40] can also be applied. In order to design different algorithms used in numerical simulations for models provided by PDEs, a finite difference method (FDM) is used to replace differential equations with difference equations. Assuming stability of the proposed numerical methods, this approach can be utilized for a wide range of practical problems [11].

This paper presents the application of PDEs, FDMs and CMLs for modeling standard and nondimensional versions of piston flow reactors (PFRs).

2. Piston Flow Reactor

2.1 Material Balance Law

In a chemical reactor design, the material balance law is used in combination with chemical kinetics and transport phenomena in order to describe the transformation of one kind of mass into another by way of a chemical reaction [41]. Let us define a control volume as a region of space with a finite volume and defined boundaries that separate this region from the rest of space. In addition, let us assume that some chemical reaction takes place within the control volume. Then, a

simple equation can be written to describe the mass balance law as follows:

$$\text{input} + \text{formation} = \text{output} + \text{accumulation},$$

where the formation part can be negative, in the case of consumption, or positive, when production as a result of a chemical reaction takes place in the system. The material balance law can also be written using volumetric flow rates and volumes as follows:

$$Q_{\text{in}}x_{\text{in}} + R_{A\,\text{avg}}V = Q_{\text{out}}x_{\text{out}} + \frac{d\left(Vx_{\text{avg}}\right)}{dt}, \tag{1}$$

where Q_{in} and Q_{out} are the volumetric inlet and outlet flow rates, respectively (volume/time), x_{in} and x_{out} are the concentration of the density of component A in the inlet and outlet flows (in moles per volume), $R_{A\,\text{avg}}$ is the spatial average of the net rate of component A formation in moles per volume over time (positive values represent production, while negative values represent consumption), V is the volume and x_{avg} is the average concentration of component A in the control volume. The expression Vx_{avg} reflects the inventory and $d\left(Vx_{\text{avg}}\right)/dt$ denotes accumulation. The reaction rate R_A describes the chemical kinetics and for the elementary reaction that transforms substance A into product B expressed as:

$$A \xrightarrow{k} B, \tag{2}$$

can be written as follows:

$$R_A = kx^p, \tag{3}$$

where k is the rate constant, x is the concentration of component A in the control volume and p is the reaction order. Subsequently, the rate constant k represents Arrhenius's law and is given by the following equation:

$$k = A\exp^{(-E_a/Rh)}, \tag{4}$$

where A is the pre-exponential or frequency factor constant for every chemical reaction (frequency of collisions), E_a is the activation energy required for the reaction (frequently expressed in J/mol), R is the universal gas constant (8.314 J/mol K) and h is the absolute temperature in kelvins (h, heating temperature).

2.2 Dynamics Equations

Figure 1 is a simple graphical representation of a PFR, where input substance A is processed into the output product B ($A \rightarrow B$). In this model, $t \in [0, T]$ denotes a temporal variable, $n \in [0, N]$ is a spatial

variable and $x(t, n)$ represents the distributed state of the process and, in practice, concentration of substance A at time step t and position n in the space of the tubular reactor. The distributed control variable of the process is given by $h(t, n)$ and represents the intensity of the heat source at time step t and spatial position n. The variable $v(t)$ denotes the velocity of the fluid. Let us assume that $n' \in [n, n + \Delta n]$ is the control volume of the PFR (Figure 2). Equation (1) can be formulated for the control volume n' as follows:

$$Q(t)x(t, n) - R_{A\,\mathrm{avg}}\Delta V = Q(t)x(t, n + \Delta n) + \Delta V \frac{\partial x(t, n')}{\partial t}. \tag{5}$$

The flow rate is expressed as $Q(t) = v(t)A_c$, where $v(t)$ is the fluid velocity and A_c denotes the section of the reactor. The control volume is given by $\Delta V = A_c \Delta n$. Taking all those definitions into account, using equation (3) and adding diffusion, the mass balance law for the control volume ΔV can be written as:

$$A_c \Delta n \frac{\partial x(t, n')}{\partial t} = v(t)A_c(x(t, n) - x(t, n + \Delta n)) + \alpha\left(\frac{\partial x(t, n + \Delta n)}{\partial n} - \frac{\partial x(t, n)}{\partial n}\right) - A_c \Delta n k x^p(t, n'). \tag{6}$$

The expression on the left side of equation (6) represents the velocity of substance A changing over time for the control volume of the reactor. The first expression on the right side denotes the amount of substance A flowing through the control volume of the reactor. The second one represents the diffusion process, while the last one denotes reaction, that is, the amount of substance A processed into output product B. Parameter α is the diffusion factor, and p signifies the reaction order. For further investigation, the first reactor order is assumed ($p = 1$). Dividing equation (6) by $A_c \Delta n$, the following equation can be obtained:

$$\frac{\partial x(t, n')}{\partial t} = -v(t)\left(\frac{x(t, n + \Delta n) - x(t, n)}{\Delta n}\right) + \frac{\alpha}{A_c}\left(\frac{\frac{\partial x(t, n+\Delta n)}{\partial n} - \frac{\partial x(t, n)}{\partial n}}{\Delta n}\right) - kx(t, n'). \tag{7}$$

Assuming that $\alpha_1 = \alpha / A_c$, using the derivative definition and applying $\Delta n \to 0$ when $n' \to n$, the mass balance law can finally be presented as follows:

$$\frac{\partial x(t, n)}{\partial t} + v(t)\frac{\partial x(t, n)}{\partial n} = \alpha_1 \frac{\partial^2 x(t, n)}{\partial n^2} - kx(t, n), \tag{8}$$

where the second expression represents advection or convection, the next one denotes diffusion and the last one describes the chemical reaction process with $k = k(h)$ and $p = 1$. The initial and boundary conditions can be defined as:

$$\begin{aligned} &\text{for } t = 0 \text{ and } 0 < n \le N: \; x(0, n) = 0, \\ &\text{for } t > 0 \text{ and } n = 0: \qquad x(t, 0) = x_t, \end{aligned} \tag{9}$$

where x_t is the instantaneous density of the substance A in the reactor's inlet.

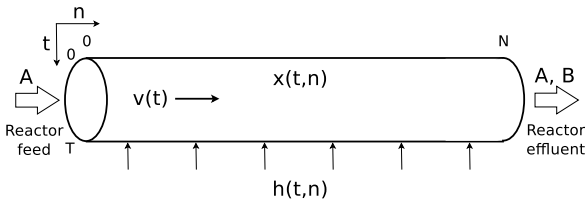

Figure 1. A PFR.

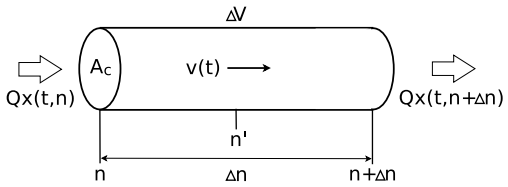

Figure 2. The control volume of a PFR.

2.3 Nondimensional Material Balance Equation

Let us assume nondimensional variables for time:

$$\theta = \frac{t}{\tau} \Rightarrow t = \frac{\theta N}{v}, \tag{10}$$

where the average flow time is given by $\tau = N/v$. The nondimensionalized spatial variable and the density of substance A are expressed as:

$$z = \frac{n}{N} \Rightarrow n = zN, \tag{11}$$

$$u = \frac{x}{x_0} \Rightarrow x = ux_0, \tag{12}$$

https://doi.org/10.25088/ComplexSystems.30.1.47

where x_0 is the initial density of substance A and can be also written as $x_0 = x(t, 0)$. Putting equations (10), (11) and (12) into equation (8), we can obtain:

$$\frac{vx_0}{N}\frac{\partial u}{\partial \theta} + \frac{vx_0}{N}\frac{\partial u}{\partial z} = \alpha_1 \frac{x_0}{N^2}\frac{\partial^2 u}{\partial z^2} - ku^p x_0^p. \tag{13}$$

Multiplying both sides by N/vx_0, the following equation can be written:

$$\frac{\partial u}{\partial \theta} + \frac{\partial u}{\partial z} = \frac{\partial^2 u}{\partial z^2}\left(\frac{\alpha_1}{vN}\right) - u^p\left(\frac{N}{v}kx_0^{p-1}\right). \tag{14}$$

Equation (13) can be also transferred to:

$$\frac{\partial u}{\partial \theta} + \frac{\partial u}{\partial z} = \frac{\partial^2 u}{\partial z^2}\frac{1}{P_e} - u^p D_a, \tag{15}$$

where

$$P_e = \frac{N^2 v}{\alpha_1 N} = \frac{N^2 / \alpha_1}{N/v} = \frac{\tau_{\text{diffusion}}}{\tau_{\text{hydrodynamics}}} \tag{16}$$

is the Péclet number and

$$D_a = \frac{N/v}{1/kx_0^{p-1}} = \frac{\tau_{\text{hydrodynamics}}}{\tau_{\text{reaction}}} \tag{17}$$

is the Damhöhler number. Finally, the nondimensional material balance equation can be written as:

$$\frac{\partial u}{\partial \theta} = \frac{1}{P_e}\frac{\partial^2 u}{\partial z^2} - \frac{\partial u}{\partial z} - D_a u^p. \tag{18}$$

2.4 Piston Flow Reactor Task Definition

The main task of the PFR described by the nondimensional material balance equation (equation (18)) can be defined as minimizing the average amount of unreacted component A in the reactor outlet:

$$q = \frac{1}{T}\int_0^T v(t)u(t, N)dt \to \min. \tag{19}$$

In order to achieve optimal q, PFR can be controlled using concentrated variables ($v(t)$ - fluid velocity, $u_0 = u(t, 0)$ - nondimensionalized density of component A in the reactor feed), as well as distributed variables such as the temperature of the heat sources $h(t, n)$. All the control variables are obviously limited, both temporarily and in their

accumulated values. This can be written as:

$$0 \le v(t) \le v_{\max}, \tag{20}$$

$$0 \le u(t, 0) \le u_{\max}, \tag{21}$$

$$u_{\text{avg}\,1} = \frac{1}{N}\int_0^N u(0, n)dn \le u_{\max a}, \tag{22}$$

$$u_{\text{avg}\,2} = \frac{1}{N}\int_0^N u(T, n)dn \le u_{\max a}, \tag{23}$$

$$0 \le h(t, n) \le h_{\max}, \tag{24}$$

$$h_{\text{avg}} = \frac{1}{TN}\int_0^T \int_0^N h(t, n)dtdn \le h_{\max a}. \tag{25}$$

These defined indicators are used in the simulation part of the paper to describe some quantitative results such as simple reactor efficiency given by q and $(u_{\text{avg}\,2} - u_{\text{avg}\,1})$ under application of different energy of heating sources h_{avg}.

3. Finite Difference Method

3.1 Numerical Algorithm

In this section, the FDM is used in order to solve equation (18) by approximating it with difference equations. Using the Euler method, the nondimensional material balance equation for $p = 1$ can be written as:

$$\frac{u_{\theta+1}^z - u_\theta^z}{\Delta\theta} = \frac{1}{P_e}\frac{u_\theta^{z+1} - 2u_\theta^z + u_\theta^{z-1}}{\Delta z^2} - \frac{u_\theta^z - u_\theta^{z-1}}{\Delta z} - ku_\theta^z. \tag{26}$$

After some basic transformations, the FDM algorithm can be expressed by:

$$u_{\theta+1}^z = u_\theta^{z-1}L + u_\theta^z C + u_\theta^{z+1}R, \tag{27}$$

where

$$C = 1 - \frac{2\Delta\theta}{\Delta z^2 P_e} - \frac{\Delta\theta}{\Delta z} - k\Delta\theta, \tag{28}$$

and

$$L = \frac{\Delta\theta}{\Delta z^2 P_e} + \frac{\Delta\theta}{\Delta z}, \tag{29}$$

$$R = \frac{\Delta\theta}{\Delta z^2 P_e}. \tag{30}$$

https://doi.org/10.25088/ComplexSystems.30.1.47

A graphical representation of the differential scheme defined by equations (27)–(30) is presented in Figure 3(a). However, this differential scheme is not stable from a numerical perspective. In order to improve its properties, the space average according to the Lax approach for the term u_t^n has to be introduced as follows [11]:

$$u_\theta^z = \frac{1}{2}\left(u_\theta^{z-1} + u_\theta^{z+1}\right). \tag{31}$$

Putting the Lax scheme into equations (27)–(30) and using simple transformations, the following numerical algorithm can be obtained:

$$u_{\theta+1}^z = u_\theta^{z-1} L + u_\theta^{z+1} R, \tag{32}$$

where

$$L = \frac{1}{2} + \frac{\Delta\theta}{2\Delta z} - \frac{k\Delta\theta}{2}, \tag{33}$$

and

$$R = \frac{1}{2} - \frac{\Delta\theta}{2\Delta z} - \frac{k\Delta\theta}{2}. \tag{34}$$

A graphical representation of equations (32)–(34) is presented in Figure 3(b).

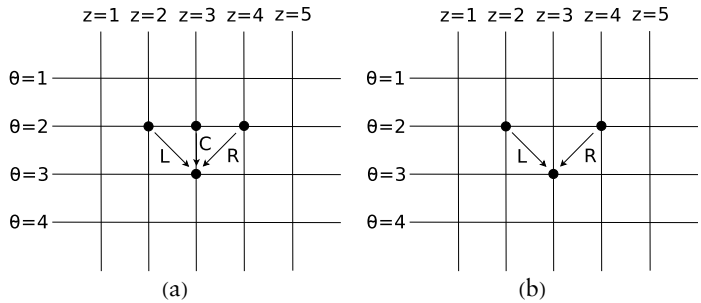

Figure 3. FDM scheme representation: (a) the basic one; (b) the Lax scheme.

3.2 Stability Analysis

Equations (32)–(34) can be also presented in the following form:

$$u_{\theta+1}^z = \left(u_\theta^{z-1} + u_\theta^{z+1}\right)\left(\frac{1}{2} - \frac{\Delta\theta}{2\Delta z} - \frac{k\Delta\theta}{2}\right) + u_\theta^{z-1}\frac{\Delta\theta}{\Delta z}. \tag{35}$$

Stability of the differential scheme can be examined by introducing the Fourier mod in accordance with the von Neumann method [11].

The Fourier mod is expressed as:

$$u = \hat{u}e^{ikx}. \tag{36}$$

Using this definition of the Fourier mod, equation (35) can be expressed as:

$$\hat{u}^{\theta+1}e^{ikx_z} = \hat{u}^{\theta}\left(e^{ikx_{z-1}} + e^{ikx_{z+1}}\right)\left(\frac{1}{2} - \frac{\Delta\theta}{2\Delta z} - \frac{k\Delta\theta}{2}\right) + \hat{u}^{\theta}e^{ikx_{z-1}}\left(\frac{\Delta\theta}{\Delta z}\right). \tag{37}$$

Dividing by e^{ikx_z} and using the fact that $\cos(k\Delta) = \left(e^{-ik\Delta} + e^{ik\Delta}\right)/2$ and $e^{ik\Delta} = \cos(k\Delta) - i\sin(k\Delta)$, we arrive at:

$$\hat{u}^{\theta+1} = \hat{u}^{\theta}\left[\cos(k\Delta)(1 - k\Delta\theta) - i\ \sin(k\Delta)\left(\frac{\Delta\theta}{\Delta z}\right)\right]. \tag{38}$$

Assuming that:

$$\hat{u}^{\theta+1} = g\hat{u}^{\theta}, \tag{39}$$

where

$$g = \cos(k\Delta)(1 - k\Delta\theta) - i\sin(k\Delta)\left(\frac{\Delta\theta}{\Delta z}\right), \tag{40}$$

according to the von Neumann approach, the condition of stability for a complex value of gain factor can be expressed as:

$$|g| = \sqrt{g^*g}\ \leq 1, \tag{41}$$

where g^* is the conjugate value of the complex number g. Taking all of this into consideration, we can write:

$$g^*g = (1 - k\Delta\theta)^2 - \sin^2(k\Delta)\left[(1 - k\Delta\theta)^2 - \left(\frac{\Delta\theta}{\Delta z}\right)^2\right]. \tag{42}$$

For $\sin^2(k\Delta) = 1$, equation (42) is expressed as:

$$g^*g = \left(\frac{\Delta\theta}{\Delta z}\right)^2, \tag{43}$$

so taking into consideration condition (41), stability is secured for an assumption that:

$$\Delta\theta \leq \Delta z. \tag{44}$$

3.3 Numerical Simulations

A numerical simulation of the PFR dynamics expressed by equation (18) can be conducted using the FDM and the Lax scheme

described in equations (32)–(34). This numerical algorithm is stable for condition (44), which has been confirmed in numerical simulations. Breaking this rule introduces instability, making the simulation impossible to perform. Parameters N, T, Δz and $\Delta\theta$ define the Euler grid itself, while the remaining parameters are part of the material balance equation in equation (18) or more precisely, in some cases, Arrhenius's law, which was given in equation (4). Simulation parameters are listed in the tables. Results of the simulation are presented in the form of plots in order to demonstrate the behavior of the system with different parameters. Moreover, each section showing the simulation results for one particular set of parameters is summarized by a table with defined factors showing the efficiency of control.

3.3.1 Experiment 1: Piston Flow Reactor without Temperature Control

Simulation parameters for this experimental case are presented in Table 1. A Gaussian distribution of component A with the parameters $\mu = 25$ and $\sigma = 10$ was introduced to the reactor feed. The distribution of the density of reactant A over time and space is visible in map form in Figure 4(a) and as a three-dimensional plot in Figure 4(b). Figure 5(a) illustrates the distribution of the density of component A in the reactor effluent as defined for time step $t = 80$. Figure 5(b) presents distribution of the density of reactant A in space for two time steps: $t = 0$ and $t = T$. Table 2 contains the values of the average density of reactant A introduced into the reactor $u_{\text{avg}\,1}$ and available at the end of the reactor $u_{\text{avg}\,2}$, the average temperature applied to the reactor h_{avg} and the quality factor q found in equation (19). The initial Gaussian distribution of reactant A flows through the reactor, but due to the low temperature delivered $h_{\text{avg}} = 0$ to the reactor in time

Parameter	Description	Value
N	space boundary	400
T	time boundary	400
Δz	space step	0.5
$\Delta\theta$	time step	0.1
μ	normal distribution, mean	25
σ	normal distribution, standard deviation	10
v	fluid velocity	1
A	frequency factor	1
E_a	activation energy	40000 (J/mol)
h	temperature	273.15 (K)
k	rate constant	$2 * 10^{-8}$
D_a	Damhöhler number	$8.97 * 10^{-6}$

Table 1. Simulation parameters for Experiment 1 (FDM).

and space, the amount of component A remains the same. The value of the quality factor q is relatively high, which does not fulfill the assumed goal.

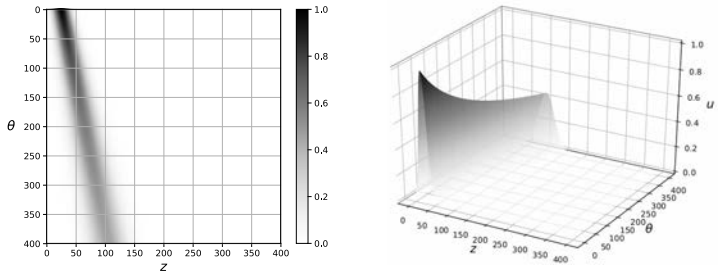

(a) (b)

Figure 4. Distribution of A over time and space in the form of: (a) map; (b) three-dimensional plot.

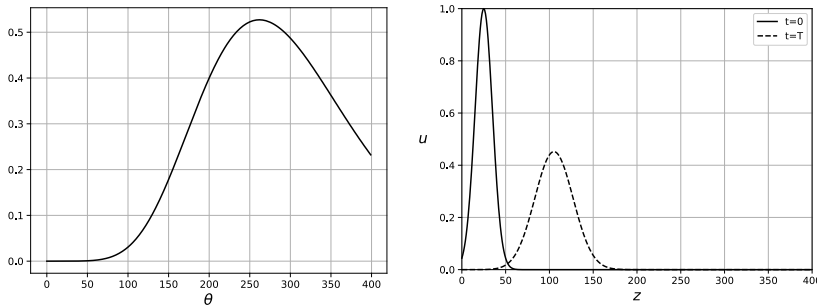

(a) (b)

Figure 5. Distribution of A: (a) over time in the reactor effluent; (b) in space for two time points.

Indicator	Description	Value
$u_{\text{avg}\,1}$	average A density in $t = 0$	0.062
$u_{\text{avg}\,2}$	average A density in $t = T$	0.062
h_{avg}	average temperature change	0 (K)
q	quality factor	0.263

Table 2. Simulation indicators for Experiment 1 (FDM).

https://doi.org/10.25088/ComplexSystems.30.1.47

3.3.2 Experiment 2: Piston Flow Reactor with Temperature Control

In this experimental case, a much higher temperature ($h = 573.15$ K) was used in order to make the reaction more efficient. The rest of the parameters remain the same. Figures 6(a) and 6(b) present the distribution of the density of reactant A over time and space in the form of a map and three-dimensional plot, respectively. Figure 7(a) illustrates the distribution of the density of component A in the reactor effluent as defined for time step $t = 80$. Figure 7(b) presents the spatial distribution of reactant A at the initial step of the simulation ($t = 0$) and at the end ($t = T$). As can be seen in Figures 6(a), 6(b) and 7(b), the initial Gaussian distribution of reactant A flows through the reactor, but this time the chemical reaction is much stronger, resulting in much higher and more efficient usage of component A. This is also confirmed by the simulation results presented in Table 3. The average density of reactant A at the end of the simulation $u_{\text{avg}\,2}$ is much lower than at the beginning of the simulation $u_{\text{avg}\,1}$.The value of the quality factor q is much lower than in the previous experimental case. Obviously, this time energy represented by the average temperature h_{avg} was much higher.

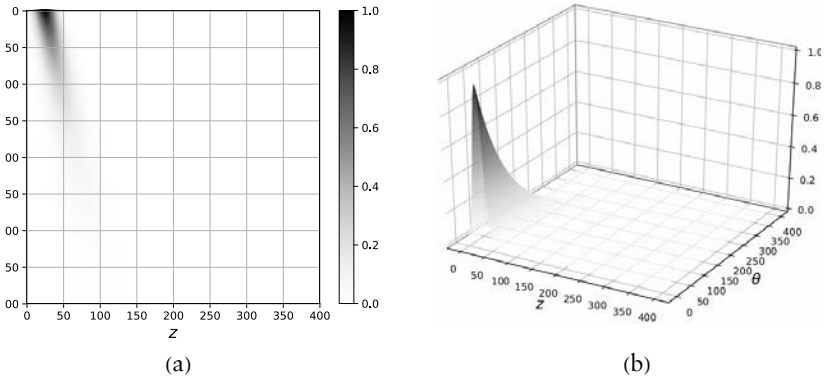

(a) (b)

Figure 6. Distribution of A over time and space in a form of: (a) map; (b) three-dimensional plot.

Indicator	Description	Value
$u_{\text{avg}\,1}$	average A density in $t = 0$	0.062
$u_{\text{avg}\,2}$	average A density in $t = T$	0.002
h_{avg}	average temp. change	300 (K)
q	quality factor	0.029

Table 3. Simulation indicators for Experiment 2 (FDM).

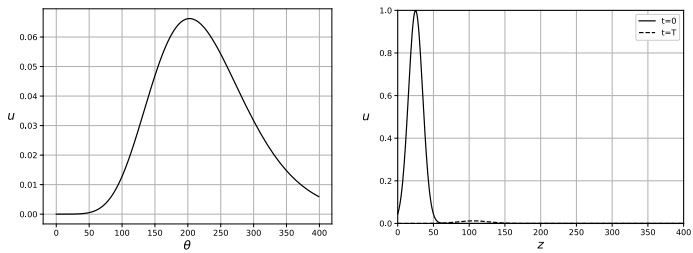

(a) (b)

Figure 7. Distribution of A: (a) over time in the reactor effluent; (b) in space for two time points.

3.3.3 Experiment 3: Dependency between the Fluid Velocity and the Quality Factor

Figure 8 presents the relationship between the quality factor q and the average temperature h_{avg} applied to the system for different fluid velocities v. As can be seen, for all tested velocities, there is a particular amount of energy in the form of heat that must be exceeded in order to achieve significant changes in the quality factor. In other words, there are particular ranges for different fluid velocities, where the relationship between the temperature and the quality factor is more or less linear. Apart from that, it can be clearly seen that the same value for the quality factor q can be achieved when the fluid velocity v grows by increasing the average temperature h_{avg}.

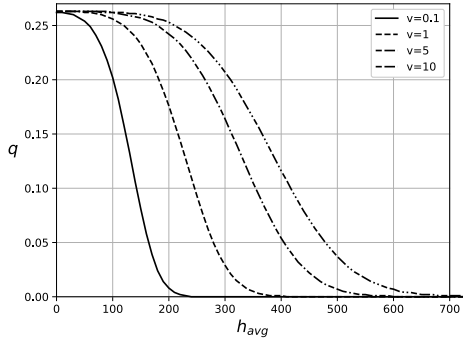

Figure 8. Dependency between the quality factor q and the average temperature h_{avg} applied to the system for different fluid velocities v, $q = f(h_{\text{avg}})$.

3.3.4 Experiment 4: Dependency between the Heating Temperature and the Quality Factor

Figure 9 illustrates the relationship between the quality factor q and the fluid velocity v for different average temperatures h_{avg} applied to the system. In general, decreasing the fluid velocity v for the same

average temperature h_{avg} reduces the quality factor q. For lower temperatures, the curve of this dependency is steeper, while for higher temperatures the dependency approaches a linear one. The same value of the quality factor q for different average temperatures h_{avg} can be achieved by changing the fluid velocity v. If the fluid velocity is higher, the temperature must also be increased in order to achieve the same value of the quality factor.

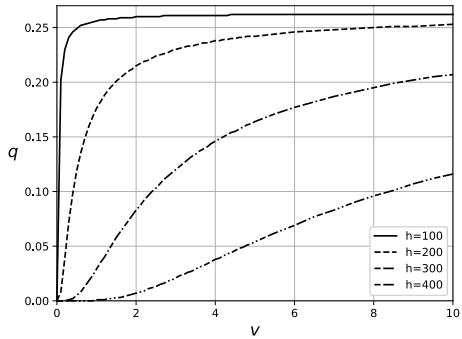

Figure 9. Dependency between the quality factor q and the fluid velocity v for different heater temperatures h, $q = f(v)$.

3.3.5 Experiment 5: Dependency between the Quality Factor and the Density of Heaters in Space

This section presents the results from examining the dependency between the quality factor q or the average amount of reactant A and the end of the simulation ($t = T$) and the density of the heaters and their temperature. Figure 10 presents the relationship between the distribution of heaters given by the distance between them in space d_s and the average heating temperature h_{avg} for different temperatures of heaters h. Obviously, the same average temperature in the system can be obtained by increasing the number of heat sources (lower distance d_s between them) if the heating temperature for each source is lower. This figure also shows that below a certain distance ($d_s \leq 5$ in this case), the amount of energy introduced into the system grows rapidly. This means that using too many sources simultaneously will cause a rapid increase in the amount of energy applied to the system. Figure 11 illustrates the dependency between the quality factor q and the distance between heaters d_s. Taking into consideration the conclusion that can be drawn by analyzing the previous chart, it can be easily seen that it is more efficient to use a higher temperature with heaters distributed more sparsely in space. The curve of the relationship between the quality factor and the distance between heaters $q = f(d_s)$

for the temperature of all heaters at the level of $h = 500$ appears to be the most linear one. This finding might be useful and valuable in practical applications. Figure 12 presents the relationship between the quality factor q and the average temperature applied to the system for different heater temperatures. As can be seen from this chart, by using higher temperatures with the heaters, it becomes easier to achieve a lower quality factor using the same amount of energy in the form of average temperature. Assuming a high temperature of the heaters (e.g., $T = 500$), increasing the average temperature applied to the system by increasing the density of heater distribution does not lead to a significant decrease in the quality factor. This essentially means that it does not make sense to introduce more sources of heat, because this will not speed up the reaction any further.

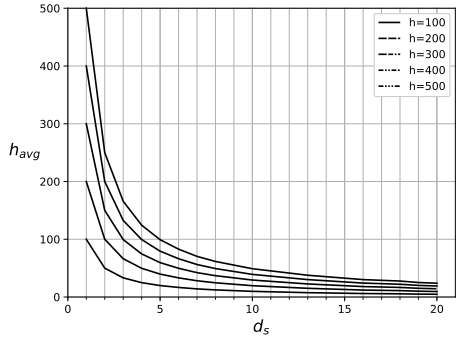

Figure 10. Dependency between average temperature h_{avg} and the distance between heaters d_s, $h_{\text{avg}} = f(d_s)$.

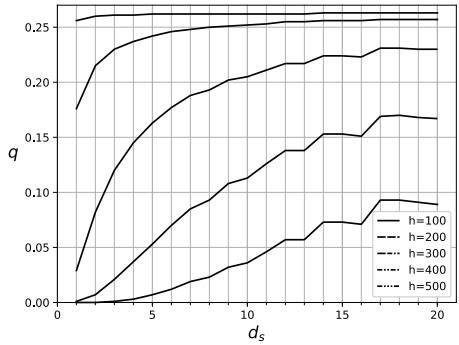

Figure 11. Dependency between the quality factor q and the distance between heaters d_s, $h_{\text{avg}} = f(d_s)$.

https://doi.org/10.25088/ComplexSystems.30.1.47

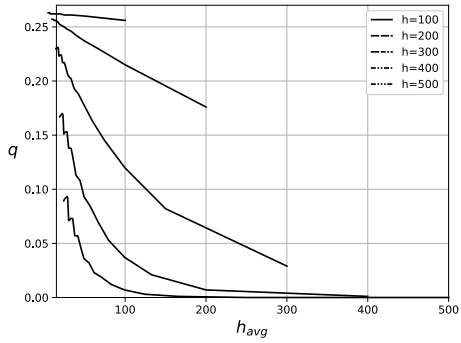

Figure 12. Dependency between the quality factor q and the average temperature h_{avg}, $q = f(h_{\text{avg}})$.

3.4 Experiment 6: Dependency between the Quality Factor and the Frequency of Heating

This section presents results that are similar to the ones presented in the previous section, but in this case the relationship between the quality factor q and the distance d_t between consecutive heating actions and the average temperature h_{avg} is considered for different temperatures h. The relationship between the quality factor and the distance in time between consecutive heating actions and the relationship between the quality factor and the average temperature applied to the system for different temperatures have a similar shape to the ones presented in the previous section, so it was decided not to present those figures. This means that both of these treatments are symmetrical. Changing the length of time or the distance in space between heating actions provides similar results. Obviously, because heating sources are inert, switching is not immediate.

4. Coupled Map Lattice

CML models are distributed parameter systems similar to CAs that can be applied to simulate spatio-temporal behavior [38–40]. In this section, this approach will be used in order to create a model of a PFR.

4.1 Mathematical Model

A one-dimensional CML can be defined as follows:

$$x_{t+1}(n) = f(x_t(n)) + \varepsilon_L g\big(x_t(n-1)\big) + \varepsilon_0 g(x_t(n)) + \varepsilon_R g\big(x_t(n+1)\big), \qquad (45)$$

where $t = 1, \ldots, T$ are discrete time steps, $n = 1, \ldots, N$ denotes the number of components, $\vec{\varepsilon} = (\varepsilon_L, \varepsilon_0, \varepsilon_R)$ is a CML kernel, $f(x)$ defines

local dynamics and $g(x)$ is a coupling function. Figure 13 is a simple graphical representation of CML assuming that $f = f(x_t(n), p_t(n))$, where $p_t(n)$ is an additional control parameter, given for each step in time and space, influencing local dynamics. In this model, periodical $(x_t(n+N) = x_t(n))$ or fixed $(x_t(0) = 0,\ x_t(N+1) = 0)$ types of boundary conditions are frequently used. The initial state of the system corresponds to the spatially distributed state of the process. CMLs, because of their capability to model distributed parameter systems and simulate complex spatio-temporal behavior, are also frequently used to model chaotic systems. An example of such a type of application is presented in Figure 14.

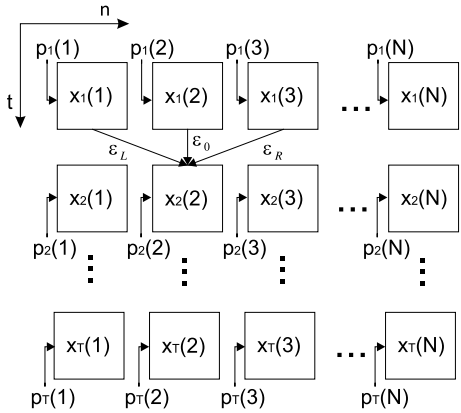

Figure 13. CML.

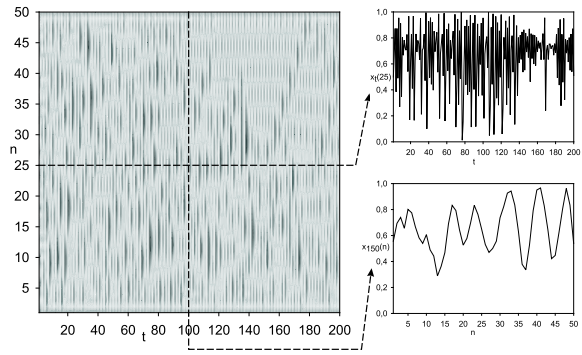

Figure 14. Chaotic spatio-temporal behavior in CML.

4.2 Numerical Algorithm

The material balance law described by equation (1) can be also formulated as follows:

$$\frac{du}{dt} = \frac{Q}{\Delta V}(u_{\text{in}} - u_{\text{out}}) - R_A, \tag{46}$$

where Q is volumetric flow defined as a product of the reactor's cross section and fluid velocity $Q = A_c v$, ΔV is a control volume defined as $\Delta V = A_c \Delta n$, where Δn is a control volume length, and u_{in} and u_{out} are the concentrations of the density of component A in the inlet and outlet flows. After some more transformations, equation (46) can be written as follows:

$$\frac{du}{dt} = \frac{v}{\Delta n}(u_{\text{in}} - u_{\text{out}}) - R_A, \tag{47}$$

where v is a velocity of fluid flowing through the reactor and $R_A = ku^p$ describes a reaction speed, where p is a reaction order (in this case $p = 1$ was assumed). Equation (47) can be presented as follows:

$$\frac{du}{dt} = \frac{v}{\Delta n}(u_{\text{in}} - u_{\text{out}}) - ku. \tag{48}$$

Using the definition of substance A density in time and space $u = u_t(n)$, in the inlet ($u_{\text{in}} = u_t(n-1)$) and outlet ($u_{\text{out}} = u_t(n+1)$) of the control volume with length $2\Delta n$ and the definition of derivative, we obtain:

$$\frac{u_{t+1}(n) - u_t(n)}{\Delta t} = \frac{v}{2\Delta n}\big(u_t(n-1) - u_t(n+1)\big) - ku_t(n). \tag{49}$$

After some basic transformations, the following equation can be derived:

$$u_{t+1}(n) = u_t(n)\big(1 - k\Delta t\big) - v\frac{\Delta t}{2\Delta n}\big(u_t(n+1) - u_t(n-1)\big). \tag{50}$$

Equation (50) describes CML with local function $f(u) = u$, coupling function $g(u) = u$ and kernel defined as:

$$\vec{\varepsilon} = \left(v\frac{\Delta t}{2\Delta n},\ 1 - k\Delta t,\ -v\frac{\Delta t}{2\Delta n}\right). \tag{51}$$

This type of kernel defines systems with reaction and nonsymmetric diffusion.

4.3 Stability Analysis

As was done for the FDM, according to the von Neumann method [11], Fourier mod $u = \hat{u}e^{ikx}$ can be introduced in order to conduct a

stability analysis. Taking into consideration that $\left(e^{ik\Delta} - e^{-ik\Delta}\right)/2 = i\sin\left(k\Delta\right)$, we obtain:

$$\hat{u}_{t+1} = \hat{u}_t\left[\left(1 - k\Delta t\right) - v\frac{\Delta t}{\Delta n} i\sin\left(k\Delta\right)\right]. \tag{52}$$

Assuming that:

$$\hat{u}_{t+1} = g\hat{u}_t, \tag{53}$$

the stability condition can be defined as follows:

$$|g| = \sqrt{g^* g} \leq 1, \tag{54}$$

where g^* is the conjugate value of the complex number g. The equation for the gain factor can written as follows:

$$|g|^2 = \left(1 - k\Delta t\right)^2 + \left(v\frac{\Delta t}{\Delta n}\sin\left(k\Delta\right)\right)^2. \tag{55}$$

For relatively small values of k and much higher values of fluid velocity v, this condition is not fulfilled, which means that the algorithm is not stable. As was done for the FDM, the spatial average of $u_t(n)$ was introduced in accordance with the Lax method:

$$u_t(n) = \frac{1}{2}\left(u_t\left(n-1\right) + u_t\left(n+1\right)\right). \tag{56}$$

A new version of the algorithm can be presented as follows:

$$\begin{aligned} u_{t+1}(n) = {} & \frac{1}{2}\left(u_t\left(n-1\right) + u_t\left(n+1\right)\right)\left(1 - k\Delta t\right) - \\ & - v\frac{\Delta t}{2\Delta n}\left(u_t\left(n+1\right) - u_t\left(n-1\right)\right). \end{aligned} \tag{57}$$

Again applying the von Neumann method [11] and taking into consideration that $\left(e^{ik\Delta} - e^{-ik\Delta}\right)/2 = i\sin\left(k\Delta\right)$ and $\left(e^{ik\Delta} + e^{-ik\Delta}\right)/2 = \cos\left(k\Delta\right)$, we obtain:

$$\hat{u}_{t+1} = \hat{u}_t\left[\left(1 - \mathrm{k}\Delta\mathrm{t}\right)\cos\left(\mathrm{k}\Delta\right) - \frac{v\Delta t}{\Delta n} i\sin\left(k\Delta\right)\right]. \tag{58}$$

The algorithm is stable for $\sqrt{g^* g} \leq 1$, so after some more transformations, the condition can be given by:

$$\frac{v\Delta t}{\Delta n} \leq 1, \tag{59}$$

which defines the stability condition for the temporal step as follows:

$$\Delta\mathrm{t} \leq \frac{\Delta n}{v}. \tag{60}$$

This type of condition defined for the temporal step is described in literature as the Courant–Friedrichs–Lewy [42, 43] condition. The CFL condition states that a time step is limited to some level given by the space step and velocity and a bigger one should not be taken.

4.4 Numerical Simulations

This section contains results of numerical simulations conducted using CML for PFR defined in previous sections for the same parameters as the ones used for the FDM.

4.4.1 Experiment 1: Piston Flow Reactor without Temperature Control

Figure 15 presents distribution of substance A over time and space, while Figure 16 shows the distribution of A over time in the reactor effluent and space for two time points. Notice that the results of the simulation are the same as using the FDM. Table 4 contains average values of substance A density in the reactor inlet $u_{\text{avg}\,1}$ and outlet $u_{\text{avg}\,2}$, average temperature applied to the reactor and quality factor defined by the equation (19). The initial Gaussian distribution of substance A flows through the reactor, but due to the small amount of energy $h_{\text{avg}} = 0$, the density of substance A remains unchanged. Both qualitative and quantitative results are the same as for the FDM.

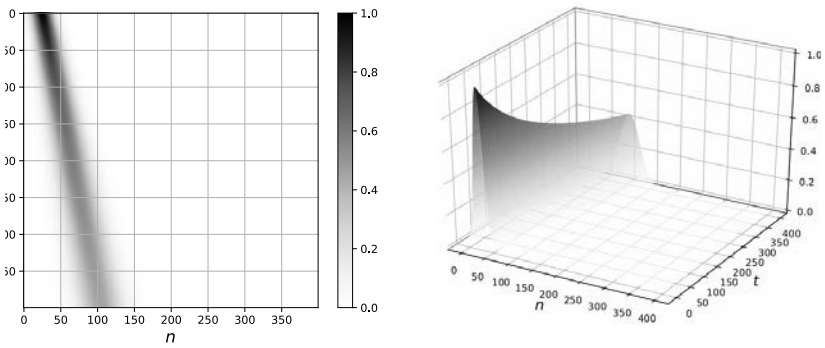

(a) (b)

Figure 15. Distribution of A over time and space in a form of: (a) map; (b) 3D plot.

4.4.2 Experiment 2: Piston Flow Reactor with Temperature Control

Figures 17 and 18 present PFR dynamics with the temperature control applied to the system. Notice that the initial amount of substance A is processed much more efficiently than it was in the previous example. Table 5 contains average values of substance A in the reactor inlet and outlet and the value of the quality factor. In order to achieve

similar simulation results, higher temperatures had to be applied in the CML model. It is related to the fact that an additional diffusion ele ment was introduced in the FDM.

Indicator	Description	Value
$u_{\text{avg}\,1}$	average A density in $t = 0$	0.062
$u_{\text{avg}\,2}$	average A density in $t = T$	0.062
h_{avg}	average temperature change	0 (K)
q	quality factor	0.263

Table 4. Simulation indicators for Experiment 1 (CML).

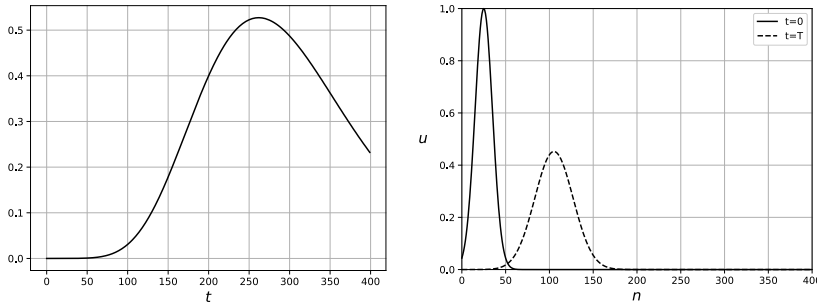

(a) (b)

Figure 16. Distribution of A: (a) over time in the reactor effluent; (b) in space for two time points.

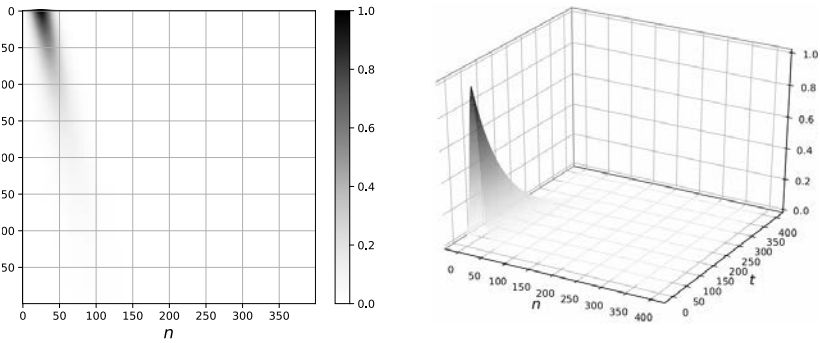

(a) (b)

Figure 17. Distribution of A over time and space in a form of: (a) map; (b) 3D plot.

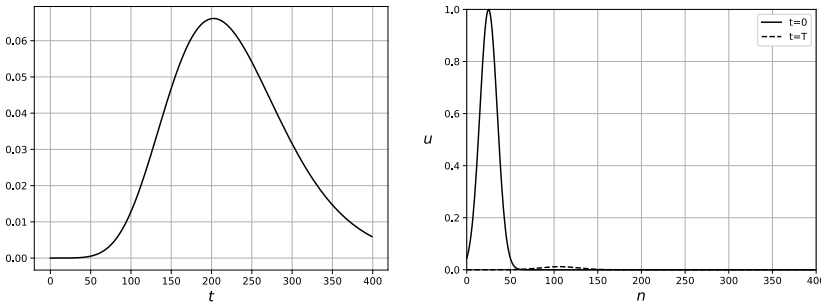

Figure 18. Distribution of A: (a) over time in the reactor effluent; (b) in space for two time points.

Indicator	Description	Value
$u_{\text{avg}\,1}$	average A density in $t = 0$	0.062
$u_{\text{avg}\,2}$	average A density in $t = T$	0.002
h_{avg}	average temperature change	1730 (K)
q	quality factor	0.029

Table 5. Simulation indicators for Experiment 2 (CML).

5. Summary

5.1 Finite Difference Method versus Coupled Map Lattice

This paper tackles the issue of modeling complex distributed parameter systems (DPSs). In this case, a chemical tubular reactor with piston flow is examined. In the first few sections, a method for formulating partial differential equations (PDEs) for a piston flow reactor (PFR) based on the material balance law and chemical kinetics is presented and a nondimensionalized version of this equation is derived. In the next step, the finite difference method (FDM) and coupled map lattice (CML) are applied in order to solve mathematical equations implementing a model of the reactor. Two simple numerical algorithms are proposed. For both of them based on the Lax approach, stability conditions are calculated using the von Neumann method. Those stability conditions are also confirmed in numerical simulations. Furthermore, a control task for such objects is defined. The following sections present the results of various experiments conducted according to the proposed models.

Based on the obtained results, it was concluded that both methods provide similar qualitative and quantitative results. However, the CML model seems to be much simpler in implementation. Moreover,

creating the mathematical model does not require deep understanding of the modeled object and the process. On the other hand, both models are similar and the biggest differences can be visible for more complicated chemical reactions introducing strong nonlinearities in the local dynamics and coupling functions. Moreover, the concept and architecture of the cellular automaton (CA) and CML seem to be more suitable to model distributed parameter systems. Such models can also be easily applied using modern, multiprocessor graphical cards, which significantly increase efficiency of simulation.

5.2 Piston Flow Reactor Properties

The main goal in controlling PFRs is to minimize the quality factor, which is defined by the amount of unreacted substance in the reactor outlet. Obviously, the amount of energy used in order to speed up the chemical reaction should be minimized. Bearing in mind that the way of providing energy in the form of heat is distributed in both time and space and that fluid velocity at the reactor inlet can be modified, this problem becomes nontrivial.

The results of Experiments 1 and 2 clearly show that by providing higher temperatures in all the heat sources along the reactor, lower values of the quality factor can be obtained. In practice, this means that in accordance with Arrhenius's law, a higher initial amount of reactant A is consumed. Unfortunately, this situation is undesirable, since it is necessary to minimize the amount of energy provided. The results of Experiment 3 confirm the fact that as the average fluid velocity in the reactor increases, more energy must be applied in order to achieve an equally low amount of reactant A in the reactor outlet. The figures included in this paper show this relationship for different fluid velocities. The results of Experiment 4 indicate that the fluid velocity must be decreased when the heating sources provide less energy. Additionally, the aim of Experiment 5 was to describe the relationship between the density of the heating sources and their temperature and the quality factor. A few interesting findings from the simulation results are worth pointing out. First, when it comes to the average spatial temperature, increasing the distance between heating sources beyond five does not change the average temperature significantly, even if the temperature of a single source is much higher. Based on the results obtained, we also state that it is more justified to use fewer heating sources or longer distance between them with more energy rather than many sources of heat with less energy. Exactly the same conclusion can be drawn for the temporal distribution of heating sources, assuming that the switching process can be done without any delays, which is not the case with objects in reality. Thus, it is more efficient to switch on heating sources less frequently with more energy.

https://doi.org/10.25088/ComplexSystems.30.1.47

References

[1] I. Aksikas, J. J. Winkin and D. Dochain, "Optimal LQ-Feedback Regulation of a Nonisothermal Plug Flow Reactor Model by Spectral Factorization," *IEEE Transactions on Automatic Control*, **52**(7), 2007 pp. 1179–1193. doi:10.1109/TAC.2007.900823.

[2] M. Baldea and P. Daoutidis, "Dynamics and Control of Autothermal Reactors for the Production of Hydrogen," *Chemical Engineering Science*, **62**(12), 2007 pp. 3218–3230. doi:10.1016/j.ces.2007.01.067.

[3] M. Li and P. D. Christofides, "Optimal Control of Diffusion-Convection-Reaction Processes Using Reduced-Order Models," *Computers and Chemical Engineering*, **32**(9), 2008 pp. 2123–2135. doi:10.1016/j.compchemeng.2007.10.018.

[4] B. Bamieh, F. Paganini and M. A. Dahleh, "Distributed Control of Spatially Invariant Systems," *IEEE Transactions on Automatic Control*, **47**(7), 2002 pp. 1091–1107. doi:10.1109/TAC.2002.800646.

[5] M. R. Jovanovic, "Modeling, Analysis, and Control of Spatially Distributed Systems," Ph.D. thesis, Mechanical Engineering, University of California, Santa Barbara, 2004.

[6] H.-X. Li and C. Qi, "Modeling of Distributed Parameter Systems for Applications: A Synthesized Review from Time–Space Separation," *Journal of Process Control*, **20**(8), 2010 pp. 891–901. doi:10.1016/j.jprocont.2010.06.016.

[7] B. Kuczewski, *Computational Aspects of Discrimination between Models of Dynamic Systems*, Zielona Góra, Poland: University of Zielona Góra Press, 2006.

[8] L. de Andrade, H. Leite and M.T.P. de Leao, "Time-Domain Distributed Parameters Transmission Line Model for Transient Analysis," *Progress in Electromagnetics Research B*, **53**, 2013 pp. 25–46. doi:10.2528/PIERB13041804.

[9] W. Qi, J. Liu and P. D. Christofides, "Distributed Supervisory Predictive Control of Distributed Wind and Solar Energy Systems," *IEEE Transactions on Control Systems Technology*, **21**(2), 2013 pp. 504–512. doi:10.1109/TCST.2011.2180907.

[10] J. M. McDonough, *Lectures In Elementary Fluid Dynamics: Physics, Mathematics and Applications*, University of Kentucky, 2009. uknowledge.uky.edu/me_textbooks/1.

[11] D. Potter, *Computational Physics*, New York: J. Wiley, 1973.

[12] S. S. E. H. Elnashaie and J. R. Grace, "Complexity, Bifurcation and Chaos in Natural and Man-Made Lumped and Distributed Systems," *Chemical Engineering Science*, **62**(13), 2007 pp. 3295–3325. doi:10.1016/j.ces.2007.02.047.

[13] R. V. Solé and J. Valls, "Order and Chaos in a 2D Lotka–Volterra Coupled Map Lattice," *Physics Letters A*, **153**(6), 1991 pp. 330–336. doi:10.1016/0375-9601(91)90954-7.

[14] R. V. Solé, J. Bascompte and J. Valls, "Nonequilibrium Dynamics in Lattice Ecosystems: Chaotic Stability and Dissipative Structures," *Chaos: An Interdisciplinary Journal of Nonlinear Science*, **2**(3), 1992 pp. 387–395. doi:10.1063/1.165881.

[15] K. M. Wagialla and S. S. E. H. Elnashaie, "Bifurcation and Complex Dynamics in Fixed-Bed Catalytic Reactors," *Chemical Engineering Science*, **50**(17), 1995 pp. 2813–2832. doi:10.1016/0009-2509(95)00042-4.

[16] Y. Orlov and D. Dochain, "Discontinuous Feedback Stabilization of Minimum-Phase Semilinear Infinite-Dimensional Systems with Application to Chemical Tubular Reactor," *IEEE Transactions on Automatic Control*, **47**(8), 2002 pp. 1293–1304. doi:10.1109/TAC.2002.800737.

[17] S. van Mourik, H. Zwart and K. J. Keesman, "Modelling and Controller Design for Distributed Parameter Systems via Residence Time Distribution," *International Journal of Control*, **82**(8), 2009 pp. 1404–1413. doi:10.1080/00207170802339426.

[18] K. Bizon, G. Continillo, L. Russo and J. Smuła, "On POD Reduced Models of Tubular Reactor with Periodic Regimes," *Computers and Chemical Engineering*, **32**(6), 2008 pp. 1305–1315. doi:10.1016/j.compchemeng.2007.06.004.

[19] P. Drag and K. Styczen, "A Two-Step Approach for Optimal Control of Kinetic Batch Reactor with Electroneutrality Condition," *Electrical Review*, **88**(6), 2012 pp. 176–180.

[20] E. Rafajłowicz, "Design of Experiments for Eigenvalue Identification in Distributed-Parameter Systems," *International Journal of Control*, **34**(6), 1981 pp. 1079–1094. doi:10.1080/00207178108922583.

[21] E. Rafajłowicz, "Optimal Experiment Design for Identification of Linear Distributed-Parameter Systems: Frequency Domain Approach," *IEEE Transactions on Automatic Control*, **28**(7), 1983 pp. 806–808. doi:10.1109/TAC.1983.1103309.

[22] E. Rafajłowicz, "Optimum Choice of Moving Sensor Trajectories for Distributed Parameter System Identification," *International Journal of Control*, **43**(5), 1986 pp. 1441–1451. doi:10.1080/00207178608933550.

[23] D. Ucinski and J. Korbicz, "Optimal Sensor Allocation for Parameter Estimation in Distributed Systems," *Journal of Inverse and Ill-Posed Problems*, **9**(3), 2001 pp. 301–318. doi:10.1515/jiip.2001.9.3.301.

[24] D. Ucinski and M. Patan, "D-Optimal Design of a Monitoring Network for Parameter Estimation of Distributed Systems," *Journal of Global Optimization*, **39**(2), 2007 pp. 291–322. doi:10.1007/s10898-007-9139-z.

[25] D. Ucinski and M. Patan, "Sensor Network Design for the Estimation of Spatially Distributed Processes," *International Journal of Applied Mathematics and Computer Science*, **20**(3), 2010 pp. 459–481. doi:10.2478/v10006-010-0034-2.

[26] J. P. Crutchfield and K. Kaneko, " Phenomenology of Spatio-temporal Chaos," *Directions in Chaos*, Vol. 1, (B.-L. Hao, ed.), Singapore: World Scientific Publishing Co., 1987. doi:10.1142/9789814415712_0008.

[27] R. G. Andrzejak, K. Lehnertz, F. Mormann, C. Rieke, P. David and C. E. Elger, "Indications of Nonlinear Deterministic and Finite-Dimensional Structures in Time Series of Brain Electrical Activity: Dependence on Recording Region and Brain State," *Physical Review E*, **64**(6), 2001 061907. doi:10.1103/PhysRevE.64.061907.

[28] S. Banerjee, A. P. Misra, P. K. Shukla and L. Rondoni, "Spatiotemporal Chaos and the Dynamics of Coupled Langmuir and Ion-Acoustic Waves in Plasmas," *Physical Review E*, **81**(4), 2010 046405. doi:10.1103/physreve.81.046405.

[29] E. Casas and F. Tröltzsch, "Optimal Sparse Boundary Control for a Semilinear Parabolic Equation with Mixed Control-State Constraints," *Control and Cybernetics*, **48**(1), 2019 pp. 89–124. http://control.ibspan.waw.pl:3000/contents/export?filename=Casas-Troeltzsch.pdf.

[30] D. Auerbach, "Controlling Extended Systems of Chaotic Elements," *Physical Review Letters*, **72**(8), 1994 pp. 1184–1187. doi:10.1103/PhysRevLett.72.1184.

[31] V. V. Astakhov, V. S. Anishchenko and A. V. Shabunin, "Controlling Spatiotemporal Chaos in a Chain of the Coupled Logistic Maps," *IEEE Transactions on Circuits and Systems*, **42**(6), 1995 pp. 352–357. doi:10.1109/81.390267.

[32] O. Beck, A. Amann, E. Schöll, J. E. S. Socolar and W. Just, "Comparison of Time-Delayed Feedback Schemes for Spatiotemporal Control of Chaos in a Reaction-Diffusion System with Global Coupling," *Physical Review E*, **66**(1), 2002 016213. doi:10.1103/PhysRevE.66.016213.

[33] A. Córdoba, M. C. Lemos and F. Jiménez-Morales, "Periodical Forcing for the Control of Chaos in a Chemical Reaction," *The Journal of Chemical Physics*, **124**(1), 2006 014707. doi:10.1063/1.2141957.

[34] P. D. Christofides, "Robust Control of Parabolic PDE Systems," *Chemical Engineering Science*, **53**(16), 1998 pp. 2949–2965. doi:10.1016/S0009-2509(98)00091-8.

[35] J. R. Weimar, *Simulation with Cellular Automata*, Berlin: Logos Verlag, 1997.

[36] B. Chopard, A. Dupuis, A. Masselot and P. Luthi, "Cellular Automata and Lattice Boltzmann Techniques: An Approach to Model and Simulate Complex Systems," *Advances in Complex Systems*, **5**(2), 2002 pp. 103–246. doi:10.1142/S0219525902000602.

[37] P. Jacewicz, *Model Analysis and Synthesis of Complex Physical Systems Using Cellular Automata*, Zielona Gora: University of Zielona Gora Press, 2003.

[38] K. Kaneko, *Theory and Applications of Coupled Map Lattices*, New York: Wiley, 1993.

[39] L. Korus, "Simple Environment for Developing Methods of Controlling Chaos in Spatially Distributed Systems," *International Journal of Applied Mathematics and Computer Science*, **21**(1), 2011 pp. 149–159. doi:10.2478/v10006-011-0011-4.

[40] L. Korus, "Efficiency Analysis of Control Algorithms in Spatially Distributed Systems with Chaotic Behavior," *International Journal of Applied Mathematics and Computer Science*, **24**(4), 2014 pp. 759–770. doi:10.2478/amcs-2014-0056.

[41] E. B. Nauman, *Chemical Reactor Design, Optimization, and Scaleup*, 2nd ed., Hoboken, NJ: Wiley, 2008.

[42] R. Courant, K. Friedrichs and H. Lewy, "Über die partiellen Differenzengleichungen der mathematischen Physik," *Mathematische Annalen*, **100**(1), 1928 pp. 32–74. doi:10.1007/BF01448839.

[43] R. Courant, K. Friedrichs and H. Lewy, "On the Partial Difference Equations of Mathematical Physics," *IBM Journal of Research and Development*, **11**(2), 1967 pp. 215–234. doi:10.1147/rd.112.0215.